Available online at website: https://jurnal.iaii.or.id/index.php/RESTI

JURNAL RESTI
(Rekayasa Sistem dan Teknologi Informasi)
Vol. 10 No. 2 (2026) 516 - 527 e-ISSN: 2580-0760

Comparative Performance of Fuzzy Logic and PID Steering Control for Improved Swerve Autonomous Vehicles

Bhakti Yudho Suprapto[1], Suci Dwijayanti[1], Ali Zainal Abidin[1], Rendyansyah[1], Oriz Djati Laksono[1], Badar Alpian[1], Muhammad Reyhan Kesuma[1]
[1]Department of Electrical Engineering, Faculty of Engineering, Universitas Sriwijaya, Inderalaya, South Sumatra, Indonesia

[*]*bhakti@ft.unsri.ac.id*

Abstract

This study presents a performance comparison of a fuzzy logic controller with a proportional-integral-derivative (PID) controller in an autonomous vehicle steering controller based on an improved swerve drive. The advantage of this swerve drive system is that it provides high maneuverability in tight spaces by utilizing nonlinear kinematic behavior and strong coupling between translational and rotational motions. This is a challenge for conventional control strategies. To overcome this problem, a fuzzy logic controller is used, which has the ability to work in more dynamic conditions. To support the control system for precision, a good structural design is required. The feasibility of the proposed improved swerve drive mechanical design is verified through finite element-based structural analysis to ensure that the control performance is not limited by mechanical constraints. Testing results show that the configuration of seven membership functions in the fuzzy logic controller provides the best performance, with an overshoot value of 7.33% and a steady-state error of 0.0324. Real-time testing of this electric vehicle prototype was conducted in five scenarios: straight road, 90° turn, parallel parking, obstacle avoidance, and on-the-spot maneuvering. The testing results also show that the fuzzy logic controller consistently outperforms the PID controller by reducing tracking error, minimizing overshoot, and achieving faster settling times, especially under complex motion conditions. Structural validation also confirms that this improved swerve drive, operating within the elastic limits of the material, supports the implementation of reliable control strategies.

Keywords: autonomous vehicle: fuzzy logic controller; improved swerve drive; motion control; PID controller

How to Cite: B. Suprapto and S. Dwijayanti, "Comparative Performance of Fuzzy Logic and PID Steering Control for Improved Swerve Autonomous Vehicles", *J. RESTI (Rekayasa Sist. Teknol. Inf.)* , vol. 10, no. 2, pp. 516 - 527, Apr. 2026.
Permalink/DOI: https://doi.org/10.29207/resti.v10i2.7594

Received: February 20, 2026
Accepted: April 19, 2026
Available Online: April 30, 2026

This is an open-access article under the CC BY 4.0 License
Published by Ikatan Ahli Informatika Indonesia

1. Introduction

The development of autonomous vehicle technology has become a strategic research focus in the era of Industrial Revolution 4.0. One crucial aspect of autonomous vehicle development is the design of a steering control system that operates optimally across a range of dynamic environmental conditions. Motion control is at the heart of many engineering systems today, from industrial robots[1] to drones navigating complex environments[2] and autonomous vehicles [3]. One innovative propulsion method developed for autonomous vehicles is the swerve drive[4]. This mechanism allows vehicles to maneuver freely because each wheel can rotate independently, making it increasingly popular in the fields of robotics and autonomous vehicles[5]. Unlike conventional wheeled systems, the swerve drive system's movement pattern is limited to forward or reverse motion. Swerve drives enable independent steering and propulsion of each wheel module, allowing the robot to move in any direction without changing its orientation[6-7]. This omnidirectional movement capability is typically used in situations that require precise positioning and agile navigation in confined, dynamic environments. This movement utilizes motors on each wheel. Even today, this omnidirectional movement exists in a type of wheel known as an omniwheel or mecanum wheel[8]. However, despite its advantages, the design and control of swerve drive systems pose significant challenges. The steering and drive motors of each wheel must be precisely coordinated to achieve smooth, stable, and accurate movement. System complexity increases with

the number of wheels, and nonlinearities in wheel dynamics, friction, and load variations further complicate control[9]. This system requires 8 motors (4 drive, 4 steer) and encoders, increasing the risk of component failure. Complex module synchronization and space utilization in the robot's corners also pose technical constraints[10]. These factors create a research problem: an effective control strategy that can handle the inherent nonlinearity and uncertainty of the swerve drive while maintaining robust and responsive motion[6], [11]. Therefore, this study improves upon the existing swerve drive by using motors integrated into the car's wheels without any gear combination. These motors are placed at the bottom, directly parallel to the wheels. The purpose of this placement is to reduce the use of additional gears that, in the long term, can potentially experience wear and require regular maintenance. Furthermore, in the direction of the steering angle, this system utilizes pulleys and belts to increase motor torque.

The movement of autonomous vehicles is not only focused on the controller but also involves mechanical components that can control position and speed to ensure precise and reliable operation. Because if the mechanical components are not precise, the control process will not run as intended. Therefore, in the design of improved Traditional control methods, such as PID controllers, have been the main solution for decades, because they are easy to understand and work well when the system dynamics are linear and predictable[12]. However, real-world systems are rarely that simple. They deal closely with nonlinear behavior, unpredictable disturbances, and uncertainties that can upset the balance of conventional controllers. Furthermore, the problem arises because these mechanical and robotic systems interact with dynamic environments, constant load changes, friction variations, and sensor noise, making it difficult to build accurate mathematical models[13]. Without precise models, traditional controllers struggle to maintain performance, often leading to overshoot, instability, or slow response. Therefore, this PID controller has been widely combined with several intelligent controllers, such as the Back Propagation Neural Network[14], Adaptive PID[15], Radial Basis Function Fuzzy PID[16], Fuzzy Self-Tuning PID[17]. This gap has prompted researchers to seek control strategies that can handle this fuzziness and ambiguity, something that is more flexible and more aligned with how humans think and make decisions. This is where fuzzy logic control comes into play.

Fuzzy logic controllers are an attractive alternative due to their ability to adapt to changing environmental conditions and handle uncertainty and non-linearity in autonomous vehicle systems[18]. This fuzzy logic controller's working process is inspired by human reasoning, using qualitative rules structured as membership functions, as well as approximate reasoning from precise numerical models[19-20]. Therefore, this approach allows the integration of expert knowledge in the form of linguistic rules, making it very suitable for complex and nonlinear systems such as motion control. This Fuzzy Controller is utilized to control the motion of a swerve drive by utilizing the motor speed and also the wheel rotation angle as input to its membership function. Specifically, the goal is to design and implement a fuzzy logic controller that can adaptively manage the motion trajectory, compensate for disturbances, and provide stable and accurate control without relying too much on precise mathematical models. A review of the existing literature reveals a growing interest in applying fuzzy logic to motion control problems. This fuzzy logic controller has been widely used in autonomous vehicles, including trajectory prediction[21], path tracking[22], pedestrian safety[23], driver safety[24], collision avoidance[25] and others.

However, research focusing on the application of fuzzy logic control as an improved swerve drive motion controller in autonomous vehicles is still limited. Furthermore, many studies in the control field sometimes neglect the feasibility of mechanical design, which can lead to impractical control performance due to structural limitations.

Therefore, this paper aims to present a performance comparison between a fuzzy logic controller and a PID controller for the improved swerve drive control in autonomous vehicles. The main contribution of this work lies in evaluating the effectiveness of fuzzy logic control in improving motion stability while ensuring the structural feasibility of the proposed improved swerve drive mechanical design through finite element-based validation.

The remainder of this paper is structured as follows. Section II presents the method, which contains the PID Controller, fuzzy logic controller, and the improved swerve drive. Section III describes the results and discussion. Section IV concludes the paper with directions for future research.

2. Methods

2.1 PID Controller

Autonomous vehicles using the improved swerve drive method proposed in this research must follow a predetermined trajectory defined in a global coordinate framework. The objective of control is to minimize the tracking error between the desired position and orientation and the actual vehicle motion, while maintaining smooth, stable wheel actuation. In this improved swerve drive, steering and actuation are independent of each wheel, exhibiting nonlinear kinematic behavior and strong coupling between translational and rotational motions. These characteristics pose problems for conventional linear control strategies, especially under variable and dynamic operating conditions and in the presence of external disturbances. Suppose the desired state vector is defined as (Equations 1-3):

$$x_d = [x_d, y_d, \theta_d]^T \quad (1)$$

and the actual state vector as

$$x = [x, y, \theta]^T \quad (2)$$

The tracking error is given by:

$$e = x_d - x \quad (3)$$

This study uses a Proportional Integral Derivative (PID) controller as the basic control strategy. PID was chosen as the controller due to its widespread use, robustness, ease of use, and simplicity. The PID controller used in this research has a structure as shown in Figure 1.

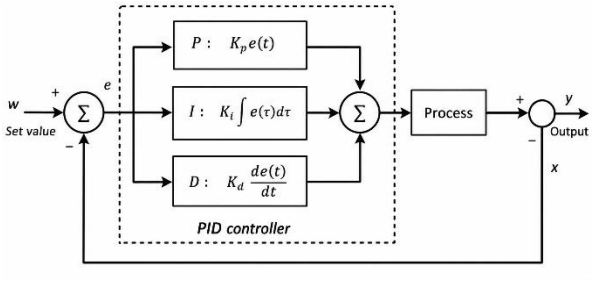


Figure 1. Block diagram of PID Controller

The PID equation can be seen in Equation 4.

$$u(t) = K_p e(t) + K_i \int e(t)dt + K_d \frac{de(t)}{dt} \quad (4)$$

K_p is the proportional gain, K_i is the integral gain, K_d is the derivative gain, and $e(t)$ is the tracking error.

This PID controller has three schemes: proportional, which aims to provide a fast response to errors between the reference value (setpoint) and the system output value. In the steering controller design for an Improved Swerve Drive-based Autonomous Vehicle, proportional control functions are used to provide immediate correction to the steering angle based on the existing error. In this system, the greater the error, the greater the control action provided to adjust the vehicle's direction. However, the main weakness of proportional control is its inability to eliminate steady-state errors and the possibility of large oscillations in the system's response. Then, integral functions to eliminate any remaining steady-state errors after using proportional control. By adding an integral component, the system can accumulate errors over time and make more accurate corrections to the steering control. In the steering control of an Improved Swerve Drive-based Autonomous Vehicle, integral control plays a role in adjusting the vehicle's steering to maintain the desired path, especially in conditions that require continuous fine adjustments. The addition of integral control helps the vehicle stay on the correct path without continuously experiencing small errors that are not corrected by proportional control alone. Meanwhile, the last is derivative, which has a function, namely, to anticipate changes in error by calculating the rate of change of error over time. This is useful in reducing oscillations and increasing system stability, especially in conditions of sudden changes in vehicle direction. In Improve Swerve Drive in Autonomous Vehicles, Derivative control helps the steering system reduce the effect of overshoot and improve adaptive response to changes in vehicle direction. The addition of Derivative control in the PID algorithm for Improve Swerve Drive helps the vehicle maintain the stability and responsiveness of the steering system, especially when facing sharp turns or sudden changes in lane.

2.2 Fuzzy Logic Controller

A fuzzy logic controller (FLC) is an approach to modeling and controlling systems that allows for uncertainty and subjectivity in decision-making. Unlike classical logic, which only recognizes true (1) and false (0), fuzzy logic allows for values that fall between the two[25]. In Figure 2, there are three main components that play an important role in the FLC function. First, the fuzzifier functions to convert numeric input into fuzzy values by mapping input variables into appropriate fuzzy sets. Next, the inference engine takes the fuzzy values generated by the fuzzifier and uses the rule base to perform reasoning, so that it can determine the appropriate control action based on the fuzzy input. Finally, the defuzzifier functions to convert the fuzzy output from the inference engine into concrete control values called crisp values that can be used to control the system.

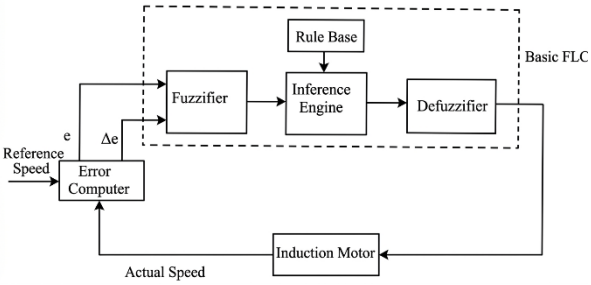


Figure 2. Block diagram of Fuzzy Logic Controller

The fuzzy logic controller is designed for the motion control of the swerve drive system. The fuzzy controller does not require an explicit mathematical model and is capable of handling nonlinearities through linguistic rules. In the Fuzzy Logic Controller method, membership functions are crucial for the system to translate crisp values into linguistic variables, or vice versa. The table below shows the membership functions used in this study, with inputs in the form of obstacle distance, obstacle position, and car position relative to the road. Meanwhile, the output of the fuzzy system is obtained through a fuzzification process, with membership functions used to regulate the PWM of the BLDC motor and the pulse step of the stepper motor. The parameters of input and output for membership functions can be seen in Tables 1-4.

This input design will be used during fuzzification, namely by determining the variables to be used, and then the membership value will be searched first. The design of this input value is obtained from the sensor reading value[26], namely distance and compass, for formula calculations. The distance parameter has variables, namely left, center, and right, for 3

membership functions. Very left, left, center, right, and very right for 5 membership functions, while for 7 membership functions, namely very left, left, near left, center, near right, right, and very right. Meanwhile, the obstacle position input variable has parameters left, middle, and right for 3 membership functions. Then for 5 membership functions: very left, left, middle, right, very right, and for 7 membership functions: very left, left, near left, middle, near right, right, and very right. The membership weight value is determined by Equation 5.

Table 1. Input Membership Function: Obstacle Distance

Distance (cm) 7 member	Distance (cm) 5 member	Distance (cm) 3 member	Variable
0 – 20	0 – 30	-	Very Close
10 – 30	10 – 60	0 – 10	Close
20 – 50	-	-	Near Close
50 - 80	30 – 110	10 – 180	Middle
50 – 120	-	-	Near Far
80 – 160	60 – 160	30 – 180	Far
120 - 180	110 - 180	-	Very Far

Table 2. Input Membership Function: Obstacle Position

Position Obstacle (º) 7 member	Position Obstacle (º) 5 member	Position Obstacle (º) 3 member	Variable
-90º – -50º	-90º – -60º	-	Very Left
-80º – -20º	-90º – -60º	-90º – -30º	Left
-50º – 0º	-	-	Near Left
-20º – +20º	-90º – -60º	-35º – +35º	Middle
0º – +50º	-	-	Near Right
+20º – +80º	6 – 8,5	+30º – +90º	Right
+50º – +90º	8 - 10	-	Very Right

Table 3. Output Membership Function: Motor Speed

Motor Speed (PWM) 7 member	Motor Speed (PWM) 5 member	Motor Speed (PWM) 3 member	Variable
80	80	-	Very Low
100	130	100	Low
140	-	-	Near Low
160	170	165	Middle
180	-	-	Near Fast
210	210	250	Fast
250	250	-	Very Fast

Table 4. Output Membership Function: Steering Angle

Steering Angle (Pulse) 7 member	Steering Angle (Pulse) 5 member	Steering Angle (Pulse) 3 member	Variable
75	75	-	Very Left
50	35	75	Left
30	-	-	Near Left
0	0	0	Center
-30	-	-	Near Right
-50	-35	-75	Right
-75	-75	-	Very Right

$$\mu(x) = \begin{cases} 0, & x \le a \text{ or } x \ge c \\ \frac{x-a}{b-a}, & a \le x \le b \\ \frac{c-x}{c-b}, & b \le x \le c \end{cases} \quad (5)$$

The stages in controller design with fuzzy logic are creating rules that must connect variables between input and output in a fuzzy set. The purpose of this rule is to obtain a stable response according to the desired parameter results. The design concept is based on the IF-THEN concept, but in this study, the system is multivariable, namely MIMO (Multiple-Input Multiple-Output), thus the concept changes by using the AND connector (IF....AND....-THEN). The output design is known as the defuzzification process, which changes the weight value for the actuator output with the parameters Motor speed and steering angle. In this output, there are variables, namely low, medium, and fast, for 3 membership functions. In 5 membership functions, there are very low, low, medium, fast, and very fast. Meanwhile, for 7 membership functions, there are very low, low, somewhat low, medium, somewhat fast, fast, and very fast. Then, for the steering angle, the variables are left, center, and right, for 3 membership functions. Very left, left, center, right, and very right for 5 membership functions, while for 7 membership functions, namely very left, left, near left, center, near right, right, and very right. Defuzzification is shown in Equation 6.

$$f = \frac{W_1.f_1 + W_2.f_2 + \cdots + W_n.f_n}{W_1 + W_2 + \cdots + W_n} \quad (6)$$

2.3 Improved Swerve Drive Design

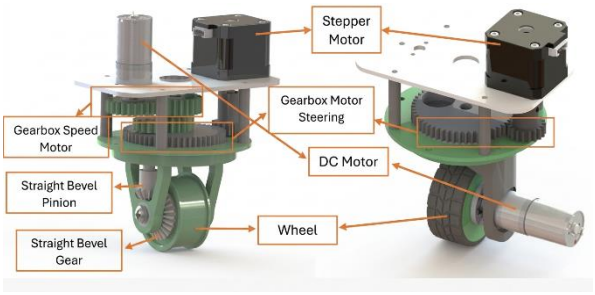
The prototype system proposed in this study uses a DC motor as the drive and a stepper motor as the steering motor. This system improves upon the existing swerve system by eliminating the gear combination in the drive motor for efficiency and simplicity. This is because swerve drive systems are known to be mechanically complex due to the extensive use of gears[27]. Figure 3 illustrates a comparison between the swerve drive system and the improved swerve drive system.

This improved swerve drive mechanism design allows autonomous vehicles to move in any direction depending on the control signal, allowing the swerve drive mechanism to be fully developed. The goal of developing the improved swerve drive design is to improve efficiency and reliability compared to conventional swerve drive designs.

In swerve drive systems, the drive motor is typically placed above the wheels, adjacent to the steering motor, connected by gears or chains. This placement makes the design taller, making the robot or autonomous vehicle body more complex, especially in terms of power transmission, as it requires additional gear mechanisms to connect the motors to the wheels.

To address this issue, the drive motor uses a DC motor, commonly found in commercially available electric motors. This motor is placed below the wheel, directly in line with the wheel. The purpose of this placement is to eliminate the use of additional gears, such as gearbox speed motor, gearbox motor steering, straight bevel pinion, and straight bevel gear, which can wear out over time and require complex routine maintenance. This improved swerve drive eliminates moving mechanical components such as gears, reducing the risk of gear maintenance and tooth wear[9], [28].

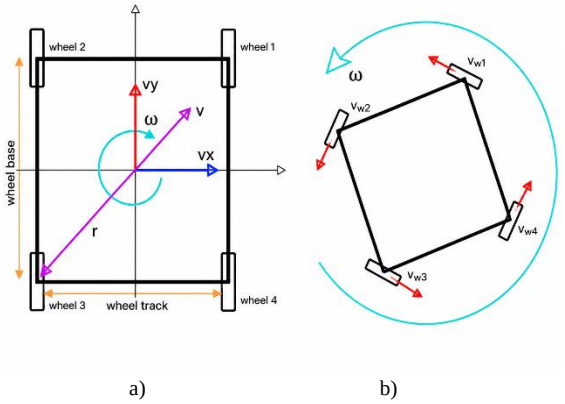
The supporting modules of the improved swerve drive are constructed using aluminum alloy and carbon fiber composite components to increase structural rigidity while minimizing weight. The mechanical structure is validated through kinematic modeling and prototype testing to ensure independent wheel rotation and smooth 360° steering capability.



a) b)

Figure 3. Swerve drive: a) swerve drive conventional b) improved swerve drive

To achieve a good design, attention must be paid to the kinematics of the swerve drive. Kinematics is a method for simplifying the inputs provided to an autonomous vehicle and maximizing the outputs to each drivetrain. This kinematic equation is used to determine the speed and direction of a wheel to enable omnidirectional maneuvering. The components involved in this kinematics calculation are the drivetrain for linear velocity and the steering kinematics for angular velocity. Figure 4 shows how the vehicle's movement mechanism is omnidirectional by approaching using the laws of geometry to calculate translation / straight motion and trigonometry to calculate the rotation and direction of the wheel.



a) b)

Figure 4. Movement of the swerve drive system (a) Translational motion (left) and, (b) rotational motion (right)

In vehicle movement modeling, there are two types of models: forward kinematics and inverse kinematics. Forward kinematics is a method for determining the final position of an object, such as a robot or vehicle, based on its initial location and movement. This technique is used to calculate the vehicle's displacement from its initial to final position by relying on data from sensors such as rotary encoders. In a swerve drive system, forward kinematics is used to determine the X and Y coordinates and direction of the vehicle based on wheel speed data. The forward kinematics equation for a swerve drive can be seen in Equation 7.

$$\begin{bmatrix} \dot{x} \\ \dot{y} \\ \dot{\omega} \end{bmatrix} = \begin{bmatrix} -\sin(\omega+\alpha_1) & cos(\omega+\alpha_1) & 2R^{-1T} \\ -\sin(\omega+\alpha_2) & cos(\omega+\alpha_2) & 2R^{-1} \\ \dots & \dots & \dots \\ -\sin(\omega+\alpha_n) & cos(\omega+\alpha_n) & 2R^{-1} \end{bmatrix} \begin{bmatrix} V_{W(1)} \\ V_{W(2)} \\ \dots \\ V_{W(n)} \end{bmatrix} \quad (7)$$

$\dot{x}$ and $\dot{y}$ are the vehicle's position coordinates, ω is the robot's orientation, or the angular velocity of the wheel, α is the orientation angle of each wheel, 2R is the distance of the wheel from the robot's center, and Vw is the linear velocity of each wheel

Meanwhile, inverse kinematics is the opposite method of forward kinematics, namely, determining the input values (wheel speed and steering angle) required for the robot to reach the desired position. In a swerve drive system, inverse kinematics is used to calculate the speed and angle of each wheel based on the desired position and speed.

In Figure 5, it can be seen that the translational speed of the robot wheel (ṽ1) is obtained from the vector addition of the robot's translational speed (ṽ) and rotational speed (ω). The inverse kinematics equations for the swerve drive are (see Equations 8-11):

$$V_x = V + \omega L \quad (8)$$

$$V_y = V + \omega W \quad (9)$$

$$V = \sqrt{V_x^2 + V_y^2} \quad (10)$$

$$\theta = tan^{-1}\left(\frac{V_y}{V_x}\right) \quad (11)$$

V_x and V_y are the vehicle's translational speeds along the X and Y axes, V is the vehicle's total speed, ω is the vehicle's rotational speed, L and W are the distances between the robot's center and the wheels along the X and Y axes, and θ is the required steering angle for each wheel.

This method allows vehicles with swerve drives to move omnidirectionally, allowing flexible maneuvering in a variety of conditions.

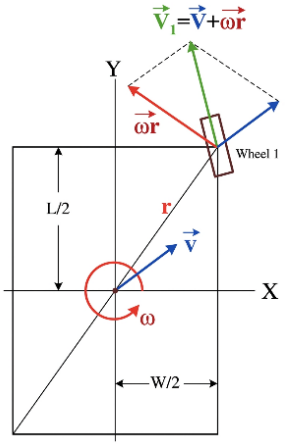


Figure 5. Vectors of wheels and a robot[19]

Furthermore, Figure 6 illustrates that the design of the control system in this study begins with initializing the system, then determining the variables to be used. The object detection stage provides two values, namely the distance and location of the object, where the objects that can be detected are cars, motorcycles, and pedestrians. Then the road segmentation process will produce the road angle and the position of the car against the results of the road segmentation. These four values will be collected and converted into Fuzzy membership functions as input to the Fuzzy Logic control system. From the control system, it will produce output in the form of an angle as input for the stepper motor and speed in the form of PWM as input for the Brushless DC.

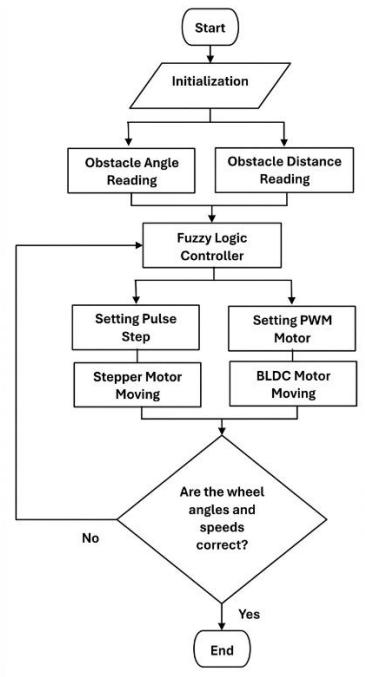


Figure 6. Flowchart of the design control system

3. Results and Discussions

This section discusses the results of simulations and testing of the swerve drive design on an Autonomous Vehicle using the Improved Swerve Drive method based on the Fuzzy Logic algorithm, which will be compared with the Proportional Integral derivative controller. The discussion covers three main aspects, namely mechanical design, which includes load analysis on the frame and wheels based on the specified load size, implementation of the Fuzzy Logic control system with variations in the number of membership functions (3, 5, and 7), and real-time testing to evaluate system performance in various vehicle maneuver scenarios.

3.1 Mechanical Design Validation

In this research, it is crucial to understand structural performance under load, particularly for wheels incorporating an improved swerve drive. Therefore, if the load on one wheel is known, the total load on the autonomous vehicle can be determined. The mechanical structure of an autonomous vehicle functions as a dynamic load support, requiring adequate strength and stiffness evaluation to ensure the safety, reliability, and service life of the system. Structural failures are caused not only by excessive loads but also by stress concentrations, excessive deformation, and inappropriate safety factor selection. Therefore, numerical analysis based on the finite element method is a crucial approach in the initial design and structural validation stages.

In this research, a static analysis of a wheel support frame was conducted using SolidWorks Simulation software. The analysis focused on evaluating total deformation, von Mises stress distribution, elastic strain, and mesh quality. The simulation results were then used to assess the feasibility of the design based on material strength criteria and international safety factor standards such as ASME and ISO. Figure 7 shows the meshing results of the model, which indicate that the mesh is quite dense and uniform, especially in the wheel area and critical joints. Good mesh quality is essential to ensure accurate simulation results. These fine tetrahedral elements indicate high accuracy in areas experiencing high stress concentrations and deformations.

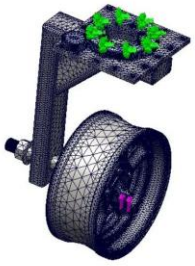


Figure 7. Mesh finite element on wheels

The mesh evaluation results indicate that the element distribution is fairly uniform, with element compaction in critical areas. This ensures that the stress and deformation results obtained are representative. However, mesh convergence analysis is still recommended to ensure that the maximum stress values are not affected by element size.

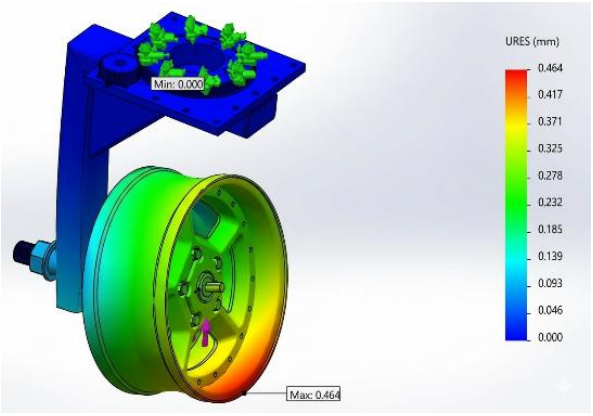


Figure 8. Simulation of the total deformation of the wheels

Figure 8 illustrates the total displacement of the structure in response to the applied load. The deformation scale is magnified 185,561 times for visual clarity. The maximum displacement occurs at the outer rim with a value of 0.648 mm, while the upper portion remains at its initial position with a displacement of 0 mm. This indicates that the greatest displacement occurs away from the fulcrum, and the greatest force affects the rim, consistent with expectations from vertical compressive forces on the rim surface. while the upper portion remains at its initial position with a displacement of 0 mm. This indicates that the greatest displacement occurs away from the fulcrum and the greatest force acts on the rim edge, in line with expectations from vertical compressive forces on the wheel surface. Meanwhile, the main frame and support areas exhibit deformations close to zero. This deformation value is relatively small compared to the overall dimensions of the structure, thus concluding that the structure has adequate stiffness and does not experience excessive deflection that could compromise system function.

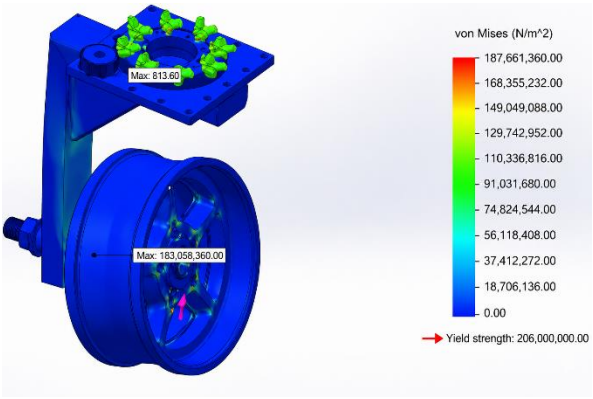


Figure 9. Von Mises stress simulation of the wheels

The stress analysis using the von Mises criterion shows the maximum stress distribution in N/m² (Pa) as shown in Figure 9. The maximum stress value recorded was 187,061,350 N/m² (187 MPa) at the wheel hub and axle hub joints. The vertical frame and top plate areas showed significantly lower stress levels. This value is still below the yield strength limit of 206 MPa, meaning the structure is theoretically safe and does not experience plastic deformation. The highest stress concentration occurs in the inner part of the wheel hub, which is the center of the load. However, the location of the maximum stress concentrated at the joints indicates a stress concentration that could potentially become a critical point of failure if the structure is subjected to dynamic or repeated cyclical loads.

3.2 PID Controller Test Results

In this research, the controller used is a PID controller with 2 sensors, namely a distance, HC-SR04 sensor, and the position or angle of the vehicle using the MPU6050 sensor. There are 2 input variables used, namely position and distance. Then the output is in the form of a PWM that will regulate the speed value of the motor wheel rotation, and also a Stepper motor that will regulate changes in the wheel angle, and input from the MPU is also used to regulate the orientation and position of the robot, and the distance sensor to read the distance to the obstacle according to the test scenario carried out. The design of the PID control system block diagram is arranged by considering the interaction between the proportional (Kp), integral (Ki), and derivative (Kd) components to the controlled plant, as in Figure 1. In the test, performance criteria such as rise time, overshoot, and steady-state error are still considered. To obtain the optimal Kp, Ki, and Kd parameters, a trial-and-error parameter tuning method and the Ziegler-Nichols plus autotuned method were used. The optimal parameters were Kp = 0.41049, Ki = 0.030024, Kd = 0.34298, with the response results as shown in Figure 10.

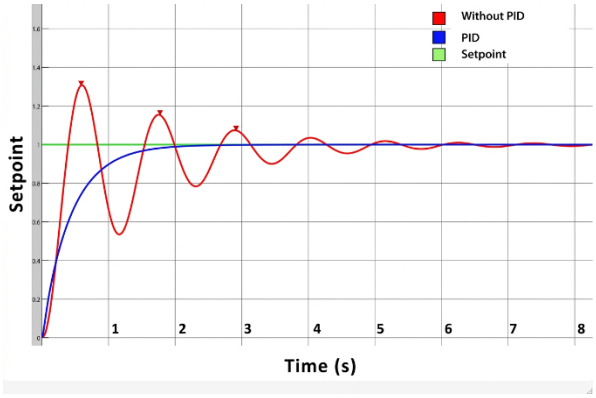


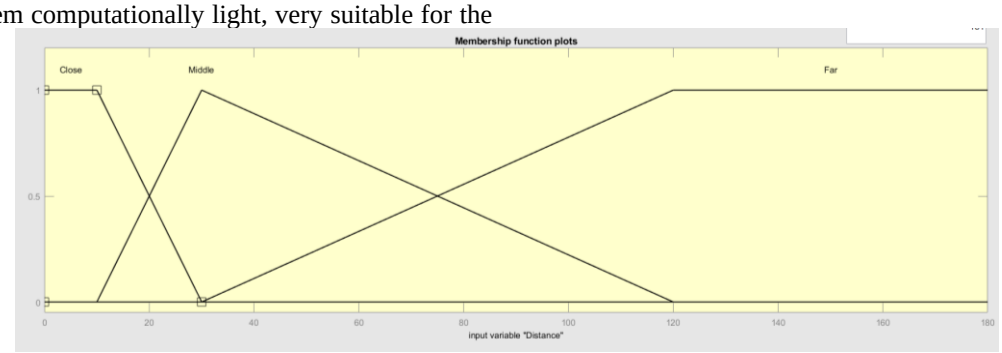
Figure 10. Comparison of simulations with and without a PID controller

The response results in Figure 10 illustrate that a performance comparison between conditions without a PID controller (red line) and with a PID controller (blue line) using parameters Kp = 0.41049, Ki = 0.030024, Kd = 0.34298. The red line shows high oscillations and unstable system response, indicating the system's inability to reach equilibrium quickly. In contrast, the blue line displays much better performance with significantly damped oscillations and shorter settling times, thanks to the implementation of PID control. The value of Kp = 0.41049 helps reduce steady-state errors, Kd = 0.34298 plays a role in damping oscillations by predicting the rate of change of error, while Ki = 0.030024 improves the offset by correcting the accumulated error over time. The combination of these three parameters results in a more stable and responsive system than without a PID, although there is still the possibility for further optimization, such as fine-tuning the Ki or Kd values to achieve smoother and more precise performance. Overall, the use of PID with these parameters has proven effective in improving motor control, reducing oscillations, and improving system accuracy.

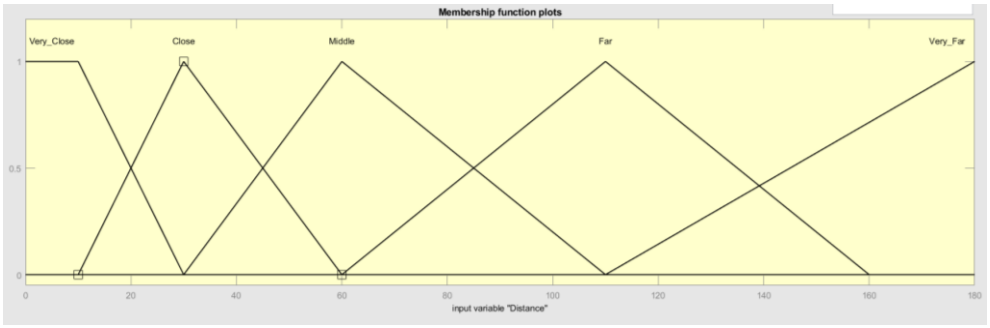
3.3 Fuzzy Logic Controller Test Results

Similar to the PID controller, the fuzzy logic controller also uses the HC-SR04 sensor as a distance sensor and the MPU6050 sensor as a position sensor. The determination of linguistic variables is combined with

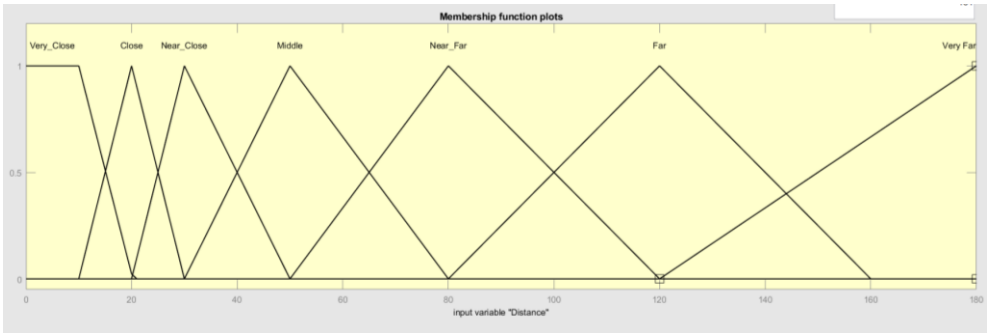
system performance evaluation. Several configurations of the number of membership functions, namely 3, 5, and 7, are tested and compared to see which one provides the most effective and stable results in controlling the vehicle. The triangular membership function and the trapezoidal membership function are chosen because they have a simple system that makes this system computationally light, very suitable for the needs of real-time systems such as autonomous vehicles. This function allows for smooth linear translation and facilitates parameter tuning. In testing the obstacle distance input, which has different membership, namely 3 membership functions, 5 membership functions, and 7 membership functions, are shown in Figures 11 and 12.



a)



b)



c)

Figure 11. Membership functions of fuzzy logic controller for distance of obstacle: a) 3 memberships, b) 5 memberships and c) 7 memberships

After the membership function is determined, the rule base is determined based on the logic of the human driver and the real situation in the field. The rule or rule base is used to determine the output of each combination of input conditions that occur. Two main inputs are used in the system, namely obstacle distance and obstacle position, each of which is given three variations in the number of membership functions: 3, 5, and 7 membership functions. These variations produce different numbers of rules according to their complexity, namely 9 rules for 3 memberships, 25 rules for 5 memberships, and 49 rules for 7 memberships. Each rule will produce two outputs at once, namely a pulse signal that regulates the direction of the steering angle and a PWM signal to regulate the motor speed. Then, testing was performed on each membership function to find the optimal response. Figure 13 illustrates that this testing can be seen in the responses.

Based on the test results as shown in Figure 13, for 3 membership functions, the system shows a very fast response with a rise time of 0.1140 seconds. However, the system performance is less stable, as seen from the very high overshoot value reaching 60.86% and a peak of 160.8640. The settling time is still acceptable at 2.2690 seconds, but the resulting steady-state error of 0.0826 indicates a significant deviation from the

reference value. This condition indicates that, despite the fast initial response, the system with 3 memberships tends to be unstable. Figure 13. a. illustrates that for 5 membership functions, there is an increase in system stability compared to 3 memberships. The overshoot decreases drastically to 37.7983% with a peak of 137.7983, and the rise time increases to 0.1928 seconds. The settling time was slightly shorter at 1.9889 seconds, and the steady-state error improved to 0.0520, as shown in Figure 13.b.

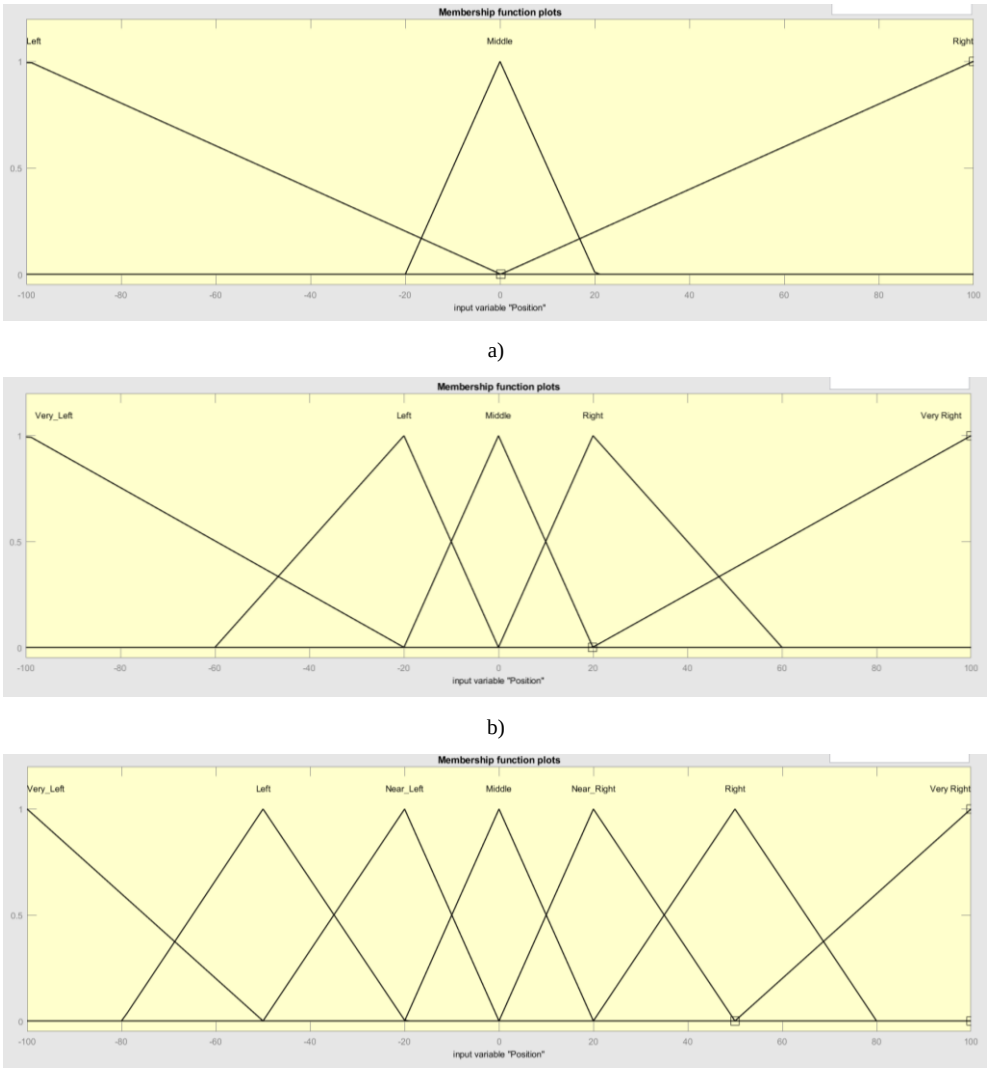


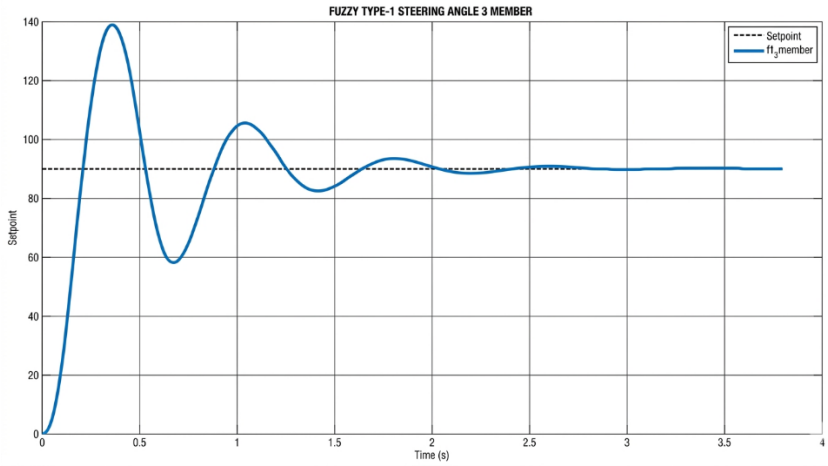
Figure 12. Membership functions of fuzzy logic controller for the position of obstacle: a) 3 memberships, b) 5 memberships, and c) 7 memberships

While these results demonstrate significant improvements in stability and accuracy, the system still exhibits suboptimal response characteristics, particularly in terms of final accuracy and smoothness of movement toward the setpoint. Meanwhile, Figure 13.c illustrates that for the 7 membership functions, the system performed better than the other configurations. Although the rise time was slightly slower at 0.3601 seconds, this was offset by a significant reduction in overshoot of 7.3372%. This value was the lowest of all tests, indicating that the system's response was much more controlled and not excessive. Furthermore, the peak value was also the smallest, at 107.3372, reinforcing the indication that the system was performing more smoothly. Indeed, the settling time was not automatically detected, likely due to small fluctuations around the final value. However, a visual inspection of the response graph indicates that the system is actually stable. The most striking feature of this configuration is the very small steady-state error value, only 0.0324. This indicates that the system is capable of following the reference value very accurately.

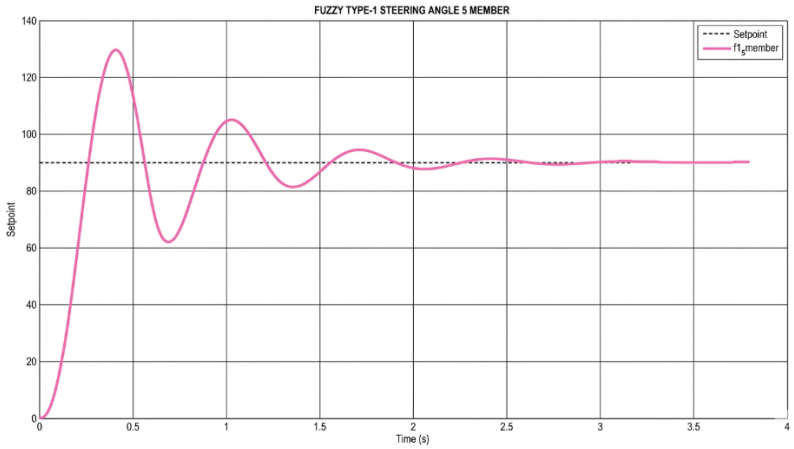
3.3 Comparison of testing with the PID controller

The test results show that the number of membership functions in the fuzzy logic controller significantly affects the performance of the steering angle control system. Testing was conducted with a setpoint of 90° to simulate the condition of the vehicle maneuvering to the right or left, as shown in Figure 14.

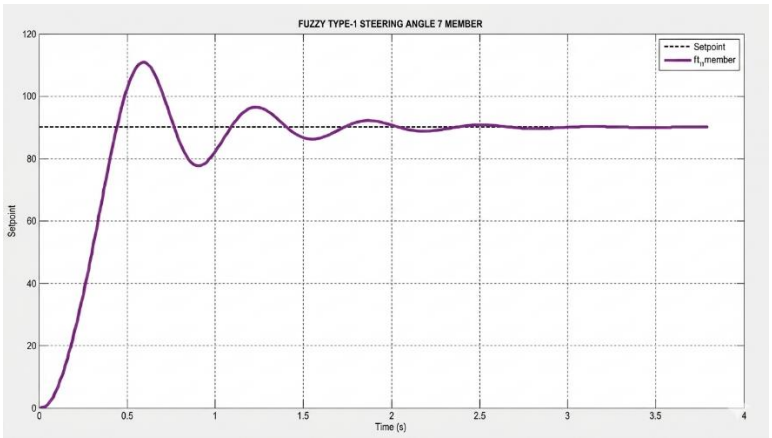
Figure 14 and Table 5 illustrate that the fuzzy configuration with 3 membership functions provided the fastest initial response with a rise time of 0.1401 seconds but resulted in the highest overshoot of 38.91% and a steady-state error of 0.0565. This indicates that although the system responded quickly, its stability and control accuracy were still low. In the 5-membership function configuration, the system showed improvements in stability with a decrease in overshoot to 29.55%, and a steady-state error of 0.0676. However, the rise time was slightly slower than that of the 3-membership functions configuration, at 0.1780 seconds. Of the three fuzzy configurations, the system with 7 membership functions produced the most optimal performance. The rise time was indeed slower, at 0.3601 seconds, but this was offset by the smallest overshoot of only 7.34%, and the lowest steady-state error of 0.0111. These characteristics reflect a smoother, more stable, and more precise system in reaching the setpoint value.



a)



b)



c)

Figure 13. Fuzzy logic response testing: a) 3 membership functions, b) 5 membership functions, c) 7 membership functions

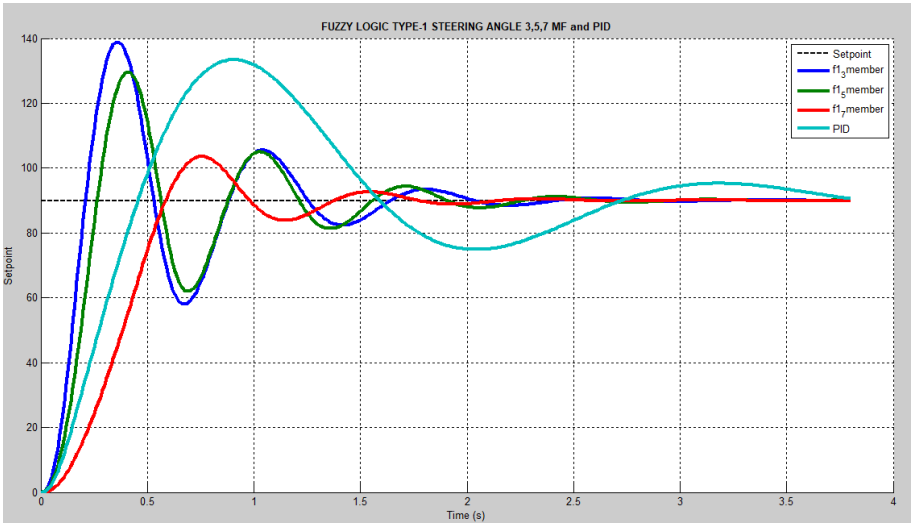


Figure 14. Comparison testing fuzzy logic 3,5,7 membership function with PID controller

For comparison, a conventional PID controller was also used, resulting in a rise time of 0.3561 seconds and an overshoot of 33.43%. Although the rise time was close to that of the 7-membership function configuration, the PID controller produced a relatively high steady-state error of 0.5465, indicating that the system still had a significant deviation from the target steering angle even when it reached steady state. These results indicate that although the PID controller is capable of providing a fast response, its final accuracy is lower than that of the fuzzy controller with 7 membership functions.

Table 5. Comparison testing parameters control fuzzy logic 3,5,7 membership function with PID controller

Parameters	3 membershp function	5 memberhip function	7 memberhip function	PID
Rise Time (s)	0,1401	0,1780	0,3601	0,3561
Peak Time (s)	0,3600	0,4100	0,6600	0,9100
Peak value	138,90	129,54	107,33	133,43
Overshoot (%)	38,91	29,55	7,34	33,43
Steady State Error	0,565	0,0676	0,011	0,5465

Therefore, it can be concluded that increasing the number of membership functions in a fuzzy controller generally improves control quality, particularly in terms of reducing overshoot, minimizing steady-state error, and providing a smoother transition to the setpoint. The fuzzy system with 7 membership functions proved superior to other fuzzy configurations and the PID controller in the tested steering angle control scenarios.

4. Conclusions

This study presents a comparative performance analysis of fuzzy logic and PID controllers for steering angle control in an enhanced swerve-driven autonomous vehicle. The results show that a fuzzy logic configuration with seven membership functions achieves the best steering angle control performance, with an overshoot of only 7.34% and a steady-state error of 0.011. Compared with configurations with three and five membership functions and a PID controller, the seven-membership fuzzy logic system exhibits higher stability and precision. This study demonstrates that increasing the number of membership functions can enrich inference capabilities and improve system control quality. Furthermore, this study also develops an enhanced swerve-driven design through mechanical design validation. Structural analysis results indicate comparable deformation and strain rates to other swerve-driven systems, despite having a lower safety factor than industrial systems. This demonstrates that the proposed design prioritizes structural efficiency and mass reduction, making it suitable for research and development-based autonomous vehicle applications. This design has sufficient strength to withstand loads up to 8,000 N, with a maximum stress of 187 MPa, well below the yield strength limit of 206 MPa for alloy steel. The recorded deformations and strains are also very small, indicating that the frame design is structurally sound and suitable for use in vehicle operations.

Future work will focus on experimental validation using an improved swerve drive platform and investigating advanced control strategies, such as adaptive controllers and Type-2 fuzzy logic, in real-time during operation. Furthermore, the integration of disturbance observers and energy-efficient control schemes will be explored to further enhance robustness and real-world applicability.

Acknowledgements

This research was supported by Universitas Sriwijaya, Competitive Research Grant In accordance with the Rector's Decree number

0028/UN9/SB3.LPPM.PT/2025 and contract number: 0108.037//UN9/SB3.LPPM.PT/2025.

References

[1] R. Zhang and X. Wei, "Research on Motion Stability Control Algorithm of Multi-axis Industrial Robot Based on Deep Reinforcement Learning," in *International Conference on Multimedia Technology and Enhanced Learning*, Springer, 2023, pp. 294–307. https://doi.org/10.1007/978-3-031-50571-3_21

[2] J. Mei *et al.*, "A high-DOF BCI control strategy mapping discrete commands to continuous motion for a drone," *IEEE Trans. Autom. Sci. Eng.*, 2025, doi: 10.1109/TASE.2025.3593497

[3] Z. B. Shaik and S. Peddakrishna, "Design and implementation of electric vehicle with autonomous motion and steering control system using single board computer and sensors," *Results Eng.*, vol. 25, p. 103995, 2025, https://doi.org/10.1016/j.rineng.2025.103995

[4] S. A. Oğuz MISIR*, Melike BEYAZLI and Z. I. Görkem Burak TAŞKIN, "Design and Mechanical Analyses of Autonomous Mobile Robot with Swerve Driving System," *Turkish J. Nat. Sci.*, vol. 13, no. 4, pp. 66–84, 2024, https://doi.org/10.46810/tdfd.1506516

[5] M. Vranas and N. J. Mourtos, "Compact Shaft-Rotating Swerve Drive with Prong Structure for Highly-Maneuverable and Agile Robots," *Athens J. Technol. Eng.*, p. 25, https://doi.org/ doi=10.30958/ajte.9-1-2

[6] B. DeNoma, M. Kendall, N. Poulos, J. Dong, and R. Frank, "Four-Wheel Independent Steering Swerve Drive for First Robotics Competition," in *ASME International Mechanical Engineering Congress and Exposition*, American Society of Mechanical Engineers, 2022, p. V005T07A076. https://doi.org/10.1115/IMECE2022-96192

[7] O. Mısır, M. Beyazlı, S. Alp, G. B. Taşkın, and Z. Isık, "Design and Mechanical Analyses of Mobile Robot with Swerve Driving System," *Türk Doğa ve Fen Derg.*, vol. 13, no. 4, pp. 66–84, 2024, doi: https://doi.org/10.46810/tdfd.1506516

[8] T. Hu, X. Xu, T.-M. Nguyen, F. Liu, S. Yuan, and L. Xie, "Tire wear aware trajectory tracking control for Multi-axle Swerve-drive Autonomous Mobile Robots," *J. Autom. Intell.*, 2025, doi: https://doi.org/10.1016/j.jai.2025.05.003

[9] H. Taheri and C. X. Zhao, "Omnidirectional mobile robots, mechanisms and navigation approaches," *Mech. Mach. Theory*, vol. 153, p. 103958, 2020, doi: https://doi.org/10.1016/j.mechmachtheory.2020.103958

[10] R. De Iaco, S. L. Smith, and K. Czarnecki, "Universally safe swerve maneuvers for autonomous driving," *IEEE Open J. Intell. Transp. Syst.*, vol. 2, pp. 482–494, 2021, doi: https://doi.org/10.1109/OJITS.2021.3138953

[11] R. Dhelika, A. F. Hadi, and P. A. Yusuf, "Development of a motorized hospital bed with swerve drive modules for holonomic mobility," *Appl. Sci.*, vol. 11, no. 23, p. 11356, 2021, doi: https://doi.org/10.3390/app112311356.

[12] L. Markina, V. Satsyk, O. Reshetylo, R. Hrudetskyi, O. Smoliankin, and N. Kuts, "Intelligent Robust Control of Ethanol Production: Advantages and Comparison with PID," in *2024 14th International Conference on Dependable Systems, Services and Technologies (DESSERT)*, IEEE, 2024, pp. 1–8. doi: 10.1109/DESSERT65323.2024.11122191

[13] K. Jia, H. Wang, D. Ren, B. Liu, Q. Zhao, and J. Hong, "A general mathematic model framework for assembly process driven digital twin of assembly precision," *J. Manuf. Syst.*, vol. 77, pp. 196–211, 2024, doi: https://doi.org/10.1016/j.jmsy.2024.09.007.

[14] L. Zhou, Q. Hu, X. Peng, and Q. Liu, "Real-Time Proportional-Integral-Derivative (PID) Tuning Based on Back Propagation (BP) Neural Network for Intelligent Vehicle Motion Control.," *Comput. Mater. Contin.*, vol. 83, no. 2, 2025, doi: https://doi.org/10.32604/cmc.2025.061894.

[15] Y. Han, M. Wang, H. Su, H. Wu, and S. Liu, "Adaptive PID control and process optimization for mandrel motion in profiled ring rolling," *J. Manuf. Process.*, vol. 145, pp. 410–425, 2025, doi: https://doi.org/10.1016/j.jmapro.2025.04.075.

[16] W. Xia, J. Yu, and Y. Dai, "Robot RBF fuzzy PID motion control based on Sine Chaos-improved particle swarm optimization," *Trans. Inst. Meas. Control*, p. 01423312251392778, 2025, doi: https://doi.org/10.1177/01423312251392778.

[17] D. Ma and J. Li, "Motion control of eight bar stamping mechanism based on fuzzy self-tuning PID," *Int. J. Model. Identif. Control*, vol. 45, no. 2–3, pp. 136–144, 2024, doi: https://doi.org/10.1504/IJMIC.2024.142275.

[18] Caroline Harry, Ahmad Rizky Amirulsyah, Harmawati Hermawati, Suci Dwijayanti, and B. Y. Suprapto, "Positioning Control System on the Movement of Wheeled Humanoid Robot Using Swerve Drive Model Based on Fuzzy Logic Controller," *J. Rekayasa Elektr.*, vol. 21, no. 1, pp. 27–35, 2025, doi: https://doi.org/10.17529/jre.v21i1.36393

[19] B. Y. Suprapto, S. Dwijayanti, and D. Amri, "Development of a position control system for wheeled humanoid robot movement using the swerve drive method based on fuzzy logic type-2," *Elektron. ir Elektrotechnika*, vol. 30, no. 1, pp. 4–13, 2024, https://doi.org/10.17529/jre.v2

[20] L. P. Wanti and L. Puspitasari, "Optimization of the Fuzzy Logic Method for Autism Spectrum Disorder Diagnosis," *J. RESTI (Rekayasa Sist. Dan Teknol. Informasi)*, vol. 6, no. 1, pp. 16–24, 2022, doi: : https://doi.org/10.29207/resti.v6i1.3599.

[21] L. Wang, X. Deng, J. Gui, and S. Wan, "Fuzzy Logic-Based Probabilistic Forecasting of Short-term Trajectory for Autonomous Vehicles," *IEEE Trans. Consum. Electron.*, 2025, doi: 10.1109/TCE.2025.3541570

[22] I. Aliskan, "The optimization-based fuzzy logic controllers for autonomous ground vehicle path tracking," *Eng. Appl. Artif. Intell.*, vol. 151, p. 110642, 2025, doi: https://doi.org/10.1016/j.engappai.2025.110642.

[23] V. Chauhan *et al.*, "Fostering fuzzy logic in enhancing pedestrian safety: Harnessing smart pole interaction unit for autonomous vehicle-to-pedestrian communication and decision optimization," *Electronics*, vol. 12, no. 20, p. 4207, 2023, doi: https://doi.org/10.3390/electronics12204207.

[24] M. A. R. Pohan, J. Utama, and B. Herdiana, "Novel Motion Planning Strategy with Fuzzy Logic for Improving Safety in Autonomous Vehicles in Response to Risky Road User Behaviors," *ASEAN J. Sci. Eng.*, vol. 4, no. 3, pp. 471–484, 2024, doi: https://doi.org/10.17509/ajse.v4i3.75343

[25] E. Samanta, S. Pal, and A. De, "Type 1 Cascaded Fuzzy Logic–Based Autonomous Vehicles Control Applications," *Controll. Des. Ind. Appl.*, pp. 309–329, 2025, doi: https://doi.org/10.1002/9781394287109.ch15.

[26] Y. Z. Maulana, F. Fathurrohman, and G. Wibisono, "Egg Incubator Temperature and Humidity Control Using Fuzzy Logic Controller," *J. RESTI (Rekayasa Sist. dan Teknol. Informasi)*, vol. 7, no. 2, pp. 318–325, 2023, doi: https://doi.org/10.29207/resti.v7i2.4728

[27] M. Haniff, H. M. Saputra, E. A. Z. Hamidi, C. H. A. H. B. Baskoro, and S. A. Pratama, "Design and control of swerve drive mechanism for autonomous mobile robot," in *2022 16th International conference on telecommunication systems, services, and applications (TSSA)*, IEEE, 2022, pp. 1–6. doi: 10.1109/TSSA56819.2022.10063871

[28] J. M. Wilson, "Development of an omnidirectional robot base with coupled steering and wheel actuation," 2023. doi: http://dx.doi.org/10.26153/tsw/45998.